



VIBRATION ANALYSIS OF A ROTATING TIMOSHENKO BEAM

S. C. LIN

*Department of Power Mechanical Engineering, National Hu-wei Institute of Technology, Hu-Wei,
632 Yunlin, Taiwan, Republic of China*

AND

K. M. HSIAO

*Department of Mechanical Engineering, National Chiao Tung University, Hsinchu, Taiwan,
Republic of China*

(Received 15 April 1999, and in final form 29 June 2000)

The governing equations for linear vibration of a rotating Timoshenko beam are derived by the d'Alembert principle and the virtual work principle. In order to capture all inertia effect and coupling between extensional and flexural deformation, the consistent linearization of the fully geometrically non-linear beam theory is used. The effect of Coriolis force on the natural frequency of the rotating beam is considered. A method based on the power series solution is proposed to solve the natural frequency of the rotating Timoshenko beam. Numerical examples are studied to verify the accuracy of the proposed method and to investigate the effect of Coriolis force on the natural frequency of rotating beams with different angular velocity, hub radius and slenderness ratio.

© 2001 Academic Press

1. INTRODUCTION

Rotating beams are often used as simple models for propellers, turbine blades, and satellite booms. The free vibration frequencies of rotating beams have been extensively studied [1–7]. Rotating beam differs from a non-rotating beam in having an additional centrifugal force and Coriolis effects on its dynamics. However, Coriolis effects were neglected in references [1, 3–6] and were considered in references [2, 7] for only Euler beam. In order to capture correctly all inertia effects and coupling between bending and stretching deformations of the beam, the equations of motion of beam might be derived by the fully geometrically non-linear beam theory [8]. However, in the conventional method [1, 3–6], the governing equations for the bending vibrations of rotating Timoshenko beam are not derived using consistent linearization of the fully geometrically non-linear beam theory. In references [1, 3–6], the beams are assumed to be linear elastic and inextensional. Thus, only bending vibrations are considered. However, in references [1, 3–6], the magnitudes of the steady state axial strain induced by the centrifugal force is not checked to verify the validity of their assumption of inextensional beam.

In this paper, exact governing equations for linear vibration of a rotating Timoshenko beam are derived based on the assumptions that the beam is linear elastic and the steady state axial strain is small. The effect of Coriolis force on the natural frequency of the rotating Timoshenko beam is considered. A method based on the power series solution to solve the

natural frequency of rotating Timoshenko beam is presented. The equations of motion for rotating Timoshenko beam are derived by the d'Alembert principle and the virtual work principle. In order to capture all inertia effect and coupling between extensional and flexural deformation, the consistent linearization [8, 9] of the fully geometrically non-linear beam theory is used in the derivation.

Numerical examples are studied to verify the accuracy of the proposed method and to investigate the effect of Coriolis force on the natural frequency of rotating beams with different angular velocity, hub radius and slenderness ratio.

2. FORMULATION

2.1. DESCRIPTION OF PROBLEM

Consider a uniform Timoshenko beam rigidly mounted on the periphery of a rigid hub of radius R rotating about its axis fixed in space at a constant angular speed, as shown in Figure 1. The deformational displacements of the beam are defined in a rotating rectangular Cartesian co-ordinate system which is rigidly tied to the hub. The origin of this co-ordinate system is chosen to be the intersection of the centroid axes of the hub and the undeformed beam. The X_1 -axis is chosen to coincide with the centroid axis of the undeformed beam, and the X_2 - and X_3 -axis are chosen to be the principal directions of the beam cross-section at the undeformed state. In this paper, all vectors are referred to this co-ordinate system. The angular velocity of the hub may be given by

$$\Omega = \{0, \Omega \sin \beta, \Omega \cos \beta\}, \quad (1)$$

where the symbol $\{ \}$ denotes a column matrix, which is used throughout the paper; β , the angle between the hub axis and the X_3 -axis, is the setting angle of the beam.

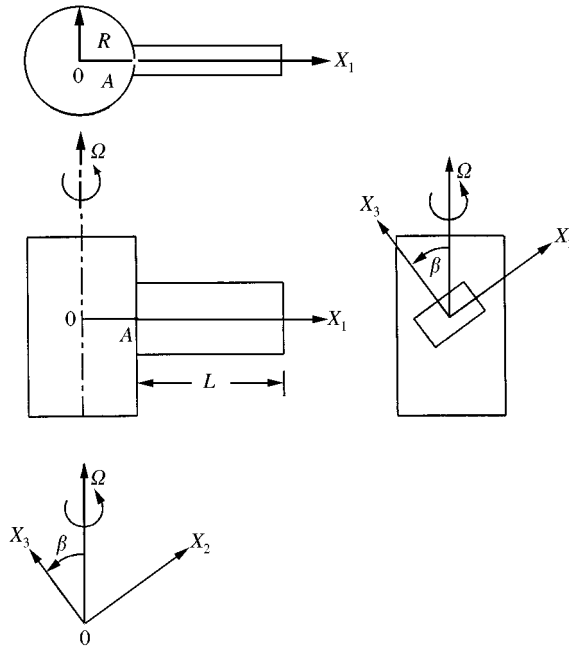


Figure 1. A rotating Timoshenko beam.

Here it is assumed that the beam is only deformed in the X_1 - X_3 plane. As mentioned in reference [2], the flapwise and lagwise bending motions are coupled for setting angles other than $\beta = 0^\circ$ and 90° . Thus, only $\beta = 0$ and 90° are considered in this study. When $\beta = 0$ and 90° , bending vibrations are flapwise and lagwise respectively. It is well known that the beam sustains a steady state axial deformations (time-independent displacement) induced by constant rotation [10]. In this study, the vibration (time-dependent displacement) of the beam is measured from the position of the steady state axial deformation, and only infinitesimal free vibration is considered. Here the engineering strain and stress are used for the measure of the strain and stress. It is assumed that the strains are small and the stress-strain relationships are linear.

2.2. KINEMATICS OF TIMOSHENKO BEAM

Let P (see Figure 2) be an arbitrary point in the beam element, and Q be the point corresponding to P on the centroid axis. The position vector of point P in the undeformed and deformed configurations may be expressed as

$$\mathbf{r}_0 = \{R + x, y, z\}, \tag{2}$$

$$\mathbf{r} = \{R + x + \bar{u}(x, t) - z \sin \varphi, y, w(x, t) + z \cos \varphi\} = r_i \mathbf{e}_i, \tag{3}$$

$$\bar{u}(x, t) = u_S(x) + u(x, t), \tag{4}$$

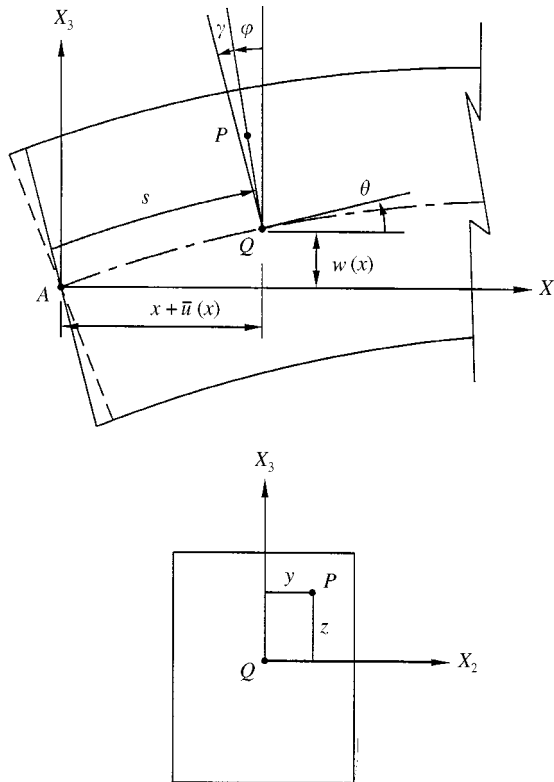


Figure 2. Kinematics of deformed Timoshenko beam.

where t is the time, $u_s(x)$ is the steady state axial deformations induced by the constant rotation, $u(x, t)$ and $w(x, t)$ are the infinitesimal displacements of point Q in the X_1 and X_3 directions, respectively, caused by the free vibration, $\varphi = \varphi(x, t)$ is the infinitesimal angle of rotation of the cross section passing through point Q about the negative X_2 -axis, caused by the free vibration, \mathbf{e}_i ($i = 1, 2, 3$) denote the unit vectors associated with the X_i -axis.

For convenience, the engineering strains in the deformed beam are obtained from the corresponding Green strains in this study. If x , y and z in equation (2) are regarded as the Lagrange co-ordinates, ε_{11} and ε_{13} , the only non-zero components of the Green strains for the Timoshenko beam, are given by [11]

$$\varepsilon_{11} = \frac{1}{2}(\mathbf{r}_{,x}^t \mathbf{r}_{,x} - 1), \quad (5)$$

$$\varepsilon_{13} = \frac{1}{2}\mathbf{r}_{,x}^t \mathbf{r}_{,z}. \quad (6)$$

From equations (3) and (4), $\mathbf{r}_{,x}$ and $\mathbf{r}_{,z}$ are expressed as

$$\mathbf{r}_{,x} = (1 + \varepsilon_0)\{\cos \theta - \kappa z \cos \varphi, 0, \sin \theta - \kappa z \sin \varphi\}, \quad (7)$$

$$\mathbf{r}_{,z} = \{-\sin \varphi, 0, \cos \varphi\}, \quad (8)$$

$$\varepsilon_0 = \frac{\partial s}{\partial x} - 1 = [(1 + \bar{u}_{,x})^2 + w_{,x}^2]^{1/2} - 1, \quad (9)$$

$$\cos \theta = \frac{\partial(x + \bar{u})}{\partial s} = \frac{1}{1 + \varepsilon_0}(1 + \bar{u}_{,x}), \quad (10)$$

$$\sin \theta = \frac{\partial w}{\partial s} = \frac{1}{1 + \varepsilon_0} w_{,x}, \quad (11)$$

$$\kappa = \frac{\partial \varphi}{\partial s} = \frac{1}{1 + \varepsilon_0} \varphi_{,x}, \quad (12)$$

where ε_0 is the unit extension of the centroid axis, θ is angle measured from the X_1 -axis to the tangent of the centroid axis. Making use of the assumption of small strain, ε_0 in equation (9) may be approximated by

$$\varepsilon_0 = \bar{u}_{,x} + \frac{1}{2}(\bar{u}_{,x}^2 + w_{,x}^2). \quad (13)$$

Substituting equations (7)–(12) into equations (5) and (6), ε_{11} and ε_{13} are given by

$$\varepsilon_{11} = \frac{1}{2}\{(1 + \varepsilon_0)^2[1 + \kappa^2 z^2 - 2\kappa z \cos(\theta - \varphi)] - 1\}, \quad (14)$$

$$\varepsilon_{13} = \frac{1}{2}(1 + \varepsilon_0) \sin(\theta - \varphi). \quad (15)$$

The engineering strain corresponding to ε_{11} and ε_{13} is given by [11]

$$\varepsilon = (1 + 2\varepsilon_{11})^{1/2} - 1, \quad (16)$$

$$\gamma = \sin^{-1}\left(\frac{2\varepsilon_{13}}{1 + \varepsilon}\right). \quad (17)$$

Note that ε and γ in equations (16) and (17) are exact expression of engineering strain for the Timoshenko beam. The exact expression of ε and γ in equations (16) and (17) are quite complicated. However, from the assumption of small strains, the approximations $\theta \approx \sin \theta$, $\cos(\theta - \varphi) \approx 1$ and $1 + \varepsilon_0 \approx 1$ may be used in the expression of ε and γ . Substituting equations (11), (12), (14) and (15) into equations (16) and (17), and using the above-mentioned approximations, ε and γ may be approximated by

$$\varepsilon = \varepsilon_0 - z\varphi_{,x}, \tag{18}$$

$$\gamma = w_{,x} - \varphi. \tag{19}$$

2.3. EQUATIONS OF MOTION

The equations of motion for rotating Timoshenko beam are derived by the d'Alembert principle and the virtual work principle. The consistent linearization of the fully geometrically non-linear beam theory is used in the derivation.

Figure 3 shows a portion of the deformed centerline of the beam. Here the generalized displacements are chosen to be \bar{u} , w , and φ defined in equation (3). The corresponding generalized forces are F_1 , F_3 , and M , the forces in X_1 , X_3 directions, and moment about negative X_2 -axis. F_{1j} , F_{3j} , and M_j ($j = 1, 2$) in Figure 3 denote the values of F_1 , F_3 , and M at sections j .

For linear elastic material, the virtual work principle may be written as

$$\delta W_{ext} = \delta W_{int}, \tag{20}$$

$$\delta W_{ext} = (F_1\delta\bar{u} + F_3\delta w + M\delta\varphi)|_1^2, \tag{21}$$

$$\delta W_{int} = E \int_{V_{12}} \delta\varepsilon^t \varepsilon dV + \alpha_s \int_{V_{12}} \delta\gamma^t \gamma dV + \rho \int_{V_{12}} \ddot{\mathbf{r}} \delta\mathbf{r} dV, \tag{22}$$

where δW_{ext} and δW_{int} are the virtual work of the external forces and the internal stresses, respectively, $()|_1^2$ is the value of $()$ in section 2 minus the value of $()$ in section 1, $\delta\varepsilon$ is the variation of ε given in equation (18), $\delta\gamma$ is the variation of γ given in equation (19), $\delta\mathbf{r}$ is the

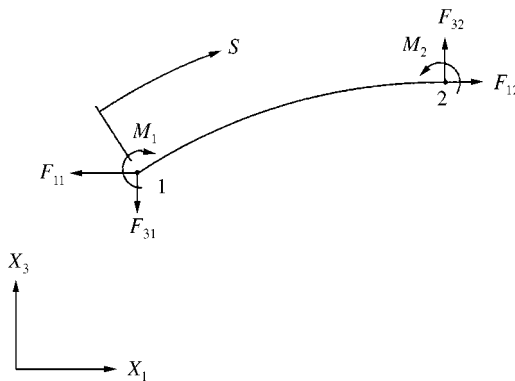


Figure 3. Free body of a portion of deformed beam.

variation of \mathbf{r} given in equation (3), and $\ddot{\mathbf{r}} = d^2\mathbf{r}/dt^2$. In this article, the symbol $(\dot{})$ denotes differentiation with respect to time t . E is Young's modulus, G is shear modulus, α_s is the shear correction factor, ρ is the density, V_{12} is the volume of the undeformed beam between sections 1 and 2. The differential volume dV may be expressed as $dV = dA dx$, where dA is the differential cross-sectional area of the beam.

Equation (21) may be equal to [12]

$$\begin{aligned} \delta W_{ext} &= \int_1^2 \frac{d}{dx} (M\delta\varphi + F_1\delta\bar{u} + F_3\delta w) dx \\ &= \int_1^2 (M_{,x}\delta\varphi + M\delta\varphi_{,x} + F_{1,x}\delta\bar{u} + F_1\delta\bar{u}_{,x} + F_{3,x}\delta w + F_3\delta w_{,x}) dx. \end{aligned} \tag{23}$$

The exact expression of δW_{int} may be very complicated. However, due to the assumption of infinitesimal vibration, the quantities u , w , and φ defined in equations (3) and (4), and their derivatives with respect to x and t are all infinitesimal quantities. For linear vibration analysis only the terms up to the first order of infinitesimal quantities are required. In order to retain all terms up to the first order of infinitesimal quantities in δW_{int} , all terms up to the first order of infinitesimal quantities are retained for $\delta\varepsilon$, ε , $\delta\gamma$, γ , $\delta\mathbf{r}$, and $\ddot{\mathbf{r}}$ in equation (21). Note that the steady state axial deformations $u_s(x)$ in equation (4) and its derivatives with respect to x are small finite quantities, not infinitesimal quantities, and are all retained as zeroth order terms of infinitesimal quantities.

From equations (3), (13), (18), and (19), $\delta\mathbf{r}$, $\delta\varepsilon$, and $\delta\gamma$ may be approximated by

$$\delta\mathbf{r} = \{\delta\bar{u} - z\delta\varphi, 0, \delta w - z\varphi\delta\varphi\}, \tag{24}$$

$$\delta\varepsilon = (1 + \bar{u}_{,x})\delta\bar{u}_{,x} + w_{,x}\delta w_{,x} - z\delta\varphi_{,x}, \tag{25}$$

$$\delta\gamma = \delta w_{,x} + \delta\varphi. \tag{26}$$

The second time derivative of \mathbf{r} in equation (3) may be expressed as

$$\ddot{\mathbf{r}} = \ddot{r}_i \mathbf{e}_i + 2\dot{r}_i \dot{\mathbf{e}}_i + r_i \ddot{\mathbf{e}}_i, \tag{27}$$

$$\dot{\mathbf{e}}_i = \boldsymbol{\Omega} \times \mathbf{e}_i, \quad \ddot{\mathbf{e}}_i = \boldsymbol{\Omega} \times \dot{\mathbf{e}}_i, \tag{28}$$

where $\boldsymbol{\Omega}$ is given in equation (1).

From equations (1), (3), (27), and (28), $\ddot{\mathbf{r}}$ in equation (27) may be approximated by

$$\ddot{\mathbf{r}} = \left\{ \begin{array}{l} \ddot{u} - z\ddot{\varphi} + 2\dot{w}\Omega \sin\beta + \Omega^2[-(R+x+\bar{u}) + z\varphi] \\ 2\Omega(\dot{u} - z\dot{\varphi})\cos\beta - y\Omega^2\cos^2\beta + \Omega^2(z+w)\sin\beta\cos\beta \\ \ddot{w} + 2\Omega(-\dot{u} + z\dot{\varphi})\sin\beta + y\Omega^2\sin\beta\cos\beta - \Omega^2(z+w)\sin^2\beta \end{array} \right\}. \tag{29}$$

Substituting equations (18), (19), (24)–(26) and (29) into equation (22), using $\int_A z dA = 0$, $\int_A yz dA = 0$, and the approximations $1 + \bar{u}_{,x} \approx 1$, and retaining all terms up to the first

order of infinitesimal quantities, one may obtain

$$\begin{aligned} \delta W_{int} = & E \int_1^2 (A\bar{u}_{,x}\delta\bar{u}_{,x} + Au_{s,x}w_{,x}\delta w_{,x} + I\varphi_{,x}\delta\varphi_{,x}) dx \\ & + \alpha_s GA \int [(w_{,x} - \varphi)\delta w_{,x} - (w_{,x} - \varphi)\delta\varphi] dx \\ & + \rho A \int_1^2 [\ddot{u} + 2\dot{w}\Omega \sin \beta - (R + x + \bar{u})\Omega^2] \delta\bar{u} dx \\ & + \rho I \int_1^2 [\ddot{\varphi} - \varphi\Omega^2 \cos^2 \beta] \delta\varphi dx \\ & + \rho A \int_1^2 [\ddot{w} - 2\dot{u}\Omega \sin \beta - w\Omega^2 \sin^2 \beta] \delta w dx, \end{aligned} \quad (30)$$

where $I = \int_A z^2 dA$ is the moment of inertia of the cross-section.

Substituting equations (23) and (30) into equation (20), and equating the terms on both sides of equation (20) corresponding to the same generalized virtual displacements, one may obtain

$$F_{1,x} = \rho A [\ddot{u} + 2\dot{w}\Omega \sin \beta - (R + x + \bar{u})\Omega^2], \quad (31)$$

$$F_{3,x} = \rho A (\ddot{w} - 2\dot{u}\Omega \sin \beta - w\Omega^2 \sin^2 \beta), \quad (32)$$

$$M_{,x} = \rho I (\ddot{\varphi} - \varphi\Omega^2 \cos^2 \beta) - \alpha_s GA (w_{,x} - \varphi), \quad (33)$$

$$M = EI\varphi_{,x}, \quad (34)$$

$$F_1 = EA\bar{u}_{,x}, \quad (35)$$

$$F_3 = EAu_{s,x}w_{,x} + \alpha_s GA (w_{,x} - \varphi). \quad (36)$$

Equations (31)–(33) are equations of motion and equations (34)–(36) are constitutive equations.

Substituting equations (34)–(36) into equations (31)–(33), one may obtain

$$AE\bar{u}_{,xx} = \rho A [\ddot{u} + \underline{2\dot{w}\Omega \sin \beta} - (R + x + \bar{u})\Omega^2], \quad (37)$$

$$AE(u_{s,x}w_{,x})_{,x} + \alpha_s GA (w_{,xx} - \varphi_{,x}) = \rho A (\ddot{w} - \underline{2\dot{u}\Omega \sin \beta} - w\Omega^2 \sin^2 \beta), \quad (38)$$

$$EI\varphi_{,xx} = \rho I (\ddot{\varphi} - \varphi\Omega^2 \cos^2 \beta) - \alpha_s GA (w_{,x} - \varphi), \quad (39)$$

where the underlined terms in equations (37) and (38) are Coriolis force. When $\beta = \pi/2$ and Ω is constant, equation (39) is identical to that given in reference [8], which is obtained by a consistent linearization of a fully non-linear beam theory. The term $\varphi\Omega^2 \cos^2 \beta$ in equation (39) is replaced by $\varphi\Omega^2$ in reference [4], where a linear beam theory is used. It can be seen that when $\beta = \pi/2$, the governing equation for rotating Timoshenko beam obtained by the linear beam theory is incorrect.

The boundary conditions for a fixed end at $x = 0$ and for a free end at $x = L$ are given by

$$u_s(0) = u(0, t) = 0, \quad w(0, t) = 0, \quad \varphi(0, t) = 0, \quad (40)$$

$$u_{s,x}(L) = u_{,x}(L, t) = 0, \quad w_{,x}(L, t) - \varphi(L, t) = 0, \quad \varphi_{,x}(L, t) = 0. \quad (41)$$

2.4. STEADY STATE AXIAL DEFORMATIONS

For the steady state axial deformations, $\bar{u}(x, t) = u_s(x)$, $u(x, t) = w(x, t) = \varphi(x, t) = 0$. Thus, equations (37)–(41) can be reduced to

$$Eu_{s,xx} = \rho(R + x + u_s)\Omega^2, \quad (42)$$

$$u_s(0) = 0, \quad u_{s,x}(L) = 0. \quad (43)$$

The solution of equation (42), which satisfies boundary conditions in equation (43) may be given by

$$u_s(x) = R \left(\cos \frac{kx}{L} - 1 \right) + \frac{L + Rk \sin k}{k \cos k} \sin \frac{kx}{L} - x, \quad k = \Omega L \sqrt{\rho/E}, \quad (44, 45)$$

where k is a dimensionless rotation speed. When $k \ll 1$, $u_s(x)$ in equation (44) may be approximated by

$$u_s(x) = \frac{\rho\Omega^2}{E} \left(\frac{-x^3}{6} - \frac{Rx^2}{2} + \frac{L^2x}{2} + RLx \right). \quad (46)$$

The centrifugal force corresponding to equation (46) is identical to that for the inextensional beam [4]. In order to compare the results with those given in the literature, k is assumed to be much smaller than unity and equation (46) is used to calculate the centrifugal force in this study.

2.5. FREE VIBRATION

The vibration of the beam is measured from the position of the steady state axial deformation. From equations (4), (37)–(39), and (42), the governing equations for free vibration may be expressed as

$$U_{,\xi\xi} = \frac{\rho L^2}{E} [\ddot{U} + \underline{2\dot{W}\Omega \sin \beta} - \Omega^2 U], \quad (47)$$

$$N_{,\xi} W_{,\xi} + N W_{,\xi\xi} + \mu_0 (W_{,\xi\xi} - \varphi_{,\xi}) = \frac{\rho L^2}{E} (-2\dot{U}\Omega \sin \beta - W\Omega^2 \sin^2 \beta + \ddot{W}), \quad (48)$$

$$\varphi_{,\xi\xi} = \frac{\rho L^2}{E} (\ddot{\varphi} - \varphi\Omega^2 \cos^2 \beta) - \mu (W_{,\xi} - \varphi), \quad (49)$$

where

$$N = k^2(-0.5\xi^2 - r\xi + r + 0.5) \tag{50}$$

$$N_{,\xi} = -k^2(\xi + r), \tag{51}$$

$$\mu_0 = \frac{\alpha_s G}{E}, \quad \mu = \eta^2 \mu_0, \quad \eta = \sqrt{AL^2/I},$$

$$\xi = \frac{x}{L}, \quad U = \frac{u}{L}, \quad W = \frac{w}{L}, \quad r = \frac{R}{L}, \tag{52}$$

and k is defined in equation (45). Note that η is the slenderness ratio of the beam, and N is the steady state axial strain. The maximum value of N occurs at the root of the beam and may be expressed as

$$\varepsilon_{max} = k^2(r + 0.5). \tag{53}$$

For linear elastic materials, it is reasonable to assume that $\varepsilon_{max} \leq 10^{-2}$.

We shall seek a solution of equations (47)–(49) in the form

$$\mathbf{U}(\xi, t) = (\mathbf{U}_R(\xi) + i\mathbf{U}_I(\xi))e^{i\omega t} \tag{54}$$

$$\mathbf{U}(\xi, t) = \{U, W, \varphi\}, \quad \mathbf{U}_R(\xi) = \{U_R, W_R, \varphi_R\}, \quad \mathbf{U}_I(\xi) = \{U_I, W_I, \varphi_I\}, \tag{55}$$

where $i = \sqrt{-1}$, and ω is the natural frequency to be determined. Introducing equation (54) into equations (47)–(49), we obtain

$$\mathbf{PA}_{,\xi\xi} + \mathbf{QA}_{,\xi} + \mathbf{RA} = \mathbf{0}, \tag{56}$$

$$\mathbf{PB}_{,\xi\xi} + \mathbf{QB}_{,\xi} + \mathbf{SB} = \mathbf{0}, \tag{57}$$

$$\mathbf{A} = \{U_R, W_I, \varphi_I\}, \quad \mathbf{B} = \{U_I, W_R, \varphi_R\}, \tag{58}$$

$$\mathbf{P} = \begin{bmatrix} 1 & 0 & 0 \\ 0 & N + \mu_0 & 0 \\ 0 & 0 & 1 \end{bmatrix}, \quad \mathbf{Q} = \begin{bmatrix} 0 & 0 & 0 \\ 0 & N_{,\xi} & -\mu_0 \\ 0 & \mu & 0 \end{bmatrix},$$

$$\mathbf{R} = \begin{bmatrix} a & d & 0 \\ d & b & 0 \\ 0 & 0 & c \end{bmatrix}, \quad \mathbf{S} = \begin{bmatrix} a & -d & 0 \\ -d & b & 0 \\ 0 & 0 & c \end{bmatrix}, \tag{59}$$

where $a = k^2 + K^2$, $b = K^2 + k^2 \sin^2 \beta$, $c = -\mu + K^2 + k^2 \cos^2 \beta$, $d = 2kK \sin \beta$, and K is a dimensionless natural frequency given by

$$K = \omega L \sqrt{\rho/E}. \tag{60}$$

It can be seen from equations (56)–(59) that $U_I = U_R$, $W_R = -W_I$, and $\varphi_R = -\varphi_I$. Thus, only equation (56) is solved in this study. In the next section, a power series method is employed to obtain the natural frequencies and vibration modes for free vibration.

2.6. POWER SERIES SOLUTION

From equations (50), (51) and (59), one can express \mathbf{P} and \mathbf{Q} in equation (59) as

$$\mathbf{P} = \mathbf{P}_0 + \zeta \mathbf{P}_1 + \zeta^2 \mathbf{P}_2, \quad \mathbf{Q} = \mathbf{Q}_0 + \zeta \mathbf{Q}_1, \tag{61}, (62)$$

where $\mathbf{P}_0, \mathbf{P}_1, \mathbf{P}_2, \mathbf{Q}_0$ and \mathbf{Q}_1 are constant matrices.

From equations (61) and (62), it can be seen that equation (56) is a set of linear ordinary differential equations with variable coefficients. The solution of equation (56) can be expressed as a power series in the independent variable ζ :

$$\mathbf{A}(\zeta) = \sum_{n=0}^{\infty} \mathbf{C}_n \zeta^n, \quad \mathbf{C}_n = \{C_{1n}, C_{2n}, C_{3n}\}, \tag{63}, (64)$$

where C_{in} ($i = 1, 2, 3$) are undetermined coefficients.

Substituting equation (63) into equation (56) and equating coefficients of like power of ζ , we obtain the recurrence formula

$$\mathbf{C}_n = \mathbf{A}_n \mathbf{C}_{n-2} + \mathbf{B}_n \mathbf{C}_{n-1}, \quad n \geq 2,$$

$$\mathbf{A}_n = \frac{-1}{n(n-1)} \begin{bmatrix} A_{11} & A_{12} & 0 \\ A_{21} & A_{22} & 0 \\ 0 & 0 & A_{33} \end{bmatrix}, \quad \mathbf{B}_n = \frac{-1}{n} \begin{bmatrix} 0 & 0 & 0 \\ 0 & B_{22} & B_{23} \\ 0 & B_{32} & 0 \end{bmatrix}, \tag{65}$$

where $A_{11} = a, A_{12} = d, A_{21} = d/f, A_{22} = \frac{1}{f}[b - (n-2)k^2 - \frac{1}{2}(n-2)(n-3)k^2], A_{33} = c, B_{22} = -(n-1)^2 k^2 r/f, B_{23} = -\mu_0/f, B_{32} = \mu,$ in which $f = \mu_0 + k^2(r + 0.5), a, b, c,$ and d are defined in equation (59).

From equation (65), it can be seen that only \mathbf{C}_0 and \mathbf{C}_1 are independent constants in equation (63), and \mathbf{C}_n can be rewritten as

$$\mathbf{C}_n = \mathbf{Y}_0^n \mathbf{C}_0 + \mathbf{Y}_1^n \mathbf{C}_1, \quad n \geq 2,$$

$$\mathbf{Y}_0^n = \mathbf{A}_n \mathbf{Y}_0^{n-2} + \mathbf{B}_n \mathbf{Y}_0^{n-1}, \quad \mathbf{Y}_1^n = \mathbf{A}_n \mathbf{Y}_1^{n-2} + \mathbf{B}_n \mathbf{Y}_1^{n-1},$$

$$\mathbf{Y}_0^0 = \mathbf{Y}_1^1 = \mathbf{I}, \quad \mathbf{Y}_0^1 = \mathbf{Y}_1^0 = \mathbf{0}, \tag{66}$$

where \mathbf{I} and $\mathbf{0}$ are unit and zero matrices of order 3×3 , respectively,

$$\mathbf{A}(\zeta) = \left(\mathbf{I} + \sum_{n=2}^{\infty} \zeta^n \mathbf{Y}_0^n \right) \mathbf{C}_0 + \left(\zeta \mathbf{I} + \sum_{n=2}^{\infty} \zeta^n \mathbf{Y}_1^n \right) \mathbf{C}_1$$

$$= \mathbf{E}_1(\zeta) \mathbf{C}_0 + \mathbf{E}_2(\zeta) \mathbf{C}_1. \tag{67}$$

From the boundary conditions given in equations (40) and (41), and equations (52), (55), (58) and (67), one can obtain

$$\mathbf{C}_0 = \mathbf{0}, \tag{68}$$

$$\mathbf{K}(K) \mathbf{C}_1 = [\mathbf{E}_{2,\zeta}(1) - \mathbf{M} \mathbf{E}_2(1)] \mathbf{C}_1 = \mathbf{0}, \tag{69}$$

where

$$\mathbf{M} = \begin{bmatrix} 0 & 0 & 0 \\ 0 & 0 & 1 \\ 0 & 0 & 0 \end{bmatrix},$$

and $\mathbf{K}(K)$ is a function of K given in equation (60).

For a non-trivial \mathbf{C}_1 , the determinant of the 3×3 matrix \mathbf{K} in equation (69) must be equal to zero. The values of K which make this determinant vanish are called eigenvalues of matrix \mathbf{K} and give the natural frequencies of the rotating Timoshenko beam through equation (60). The bisection method is used here to find the eigenvalues. Let K_i and \mathbf{X} denote an eigenvalue and the corresponding eigenvector of equation (69). The eigenvector \mathbf{X} may be obtained by solving the following standard eigenvalue problem:

$$[\mathbf{K}(K_i) + \mathbf{I}]\mathbf{X} = \lambda\mathbf{X}, \quad (70)$$

where \mathbf{I} is a unit matrix of order 3×3 . It can be seen that $\lambda = 1$ is an eigenvalue of equation (70). The eigenvector of equation (70) corresponding to $\lambda = 1$ is the required eigenvector of equation (69). Here an inverse power method is used to find the eigenvalue and eigenvector of equation (70).

Substituting equation (68) and $\mathbf{C}_1 = \mathbf{X}$ into equation (67), the mode shape corresponding to K_i can be obtained.

3. NUMERICAL EXAMPLES

To verify the accuracy of the present method and investigate the effect of the Coriolis force on the natural frequency of the rotating beam, several numerical examples are studied. Here cases with and without considering the Coriolis force, referred to as cases A and B, respectively, are considered, and the corresponding results are referred as to Present-A and Present-B respectively.

In order to compare present results with those reported in the literature, in which the linear beam theory is used and the Coriolis effect is not considered, the dimensionless natural frequency $A = \eta K = \omega L^2 \sqrt{\rho A/EI}$ and dimensionless rotational speed $\alpha = \eta k = \Omega L^2 \sqrt{\rho A/EI}$ are also employed here. While most analytical studies reported in the literature do not provide the experimental results, limited experimental measurements on the fundamental frequency under several rotating speeds are given in reference [1]. The experimental evidence did back up the predicted analytical results.

With the consideration of the Coriolis force, except $\beta = 0$ or $k = 0$, the axial and lateral vibrations are coupled in the vibration modes. However, for convenience, the dimensionless natural frequencies are divided into $K_i(A_i)$ and $K_i^z(A_i^z)$, where $K_i(A_i)$ and $K_i^z(A_i^z)$ denote the i th dimensionless natural frequencies of lateral and axial vibration, respectively, at $k = 0$.

The dimensionless natural frequencies of the rotating beams with dimensionless variables $r = 3$, $\eta k = 10$, and $\mu_0 = 0.32693$ are listed in Table 1. As expected, for $\beta = 0^\circ$ the results of Present-A, Present-B and those reported in the literature are in close agreement. For $\beta = 90^\circ$, the results of Present-B and those reported in the literature are in close agreement, but the discrepancy between the results of Present-A and Present-B are remarked. It is interesting to note that the governing equations of the Present-B for lateral vibration

TABLE 1

Dimensionless frequencies for rotating Timoshenko beam ($\alpha = \eta k = 10, r = 3, \mu_0 = 0.32693$)

β	$\eta = 10$				$\eta = 20$				
	A_1	A_2	A_3	A_4	A_1	A_2	A_3	A_4	
0°	A	22.938	44.781	66.287	71.967	23.491	55.984	96.913	143.71
	B	22.938	44.791	66.287	71.967	23.491	55.984	96.913	143.71
	C	23.050	45.598	67.716	73.076	23.524	56.105	97.188	144.49
	D	22.938	44.781	66.287	71.967	23.491	55.984	96.913	143.71
	E	23.037	45.428	66.854	72.313	23.514	56.072	97.011	143.82
90°	A	8.500	29.152	49.372	74.141	16.491	37.751	91.041	140.98
	B	20.853	44.957	66.677	71.985	21.298	55.240	96.594	143.50
	C	20.867	45.115	67.520	72.756	21.313	55.284	96.747	144.21
	D	20.753	44.315	66.109	71.620	21.277	55.162	96.473	143.43
	E	20.850	44.955	66.668	71.982	21.302	55.250	96.570	143.53

Note: A: Present-A; B: Present-B; C: reference [3]; D: reference [4]; E: reference [1].

(equations (38) and 39)) are identical to those given in reference [4] for $\beta = 0$. Thus, the Present-B results are the same as those given in reference [4] for $\beta = 0$. However, equation (39) of the Present-B for lateral vibration is different from that given in reference [4] for $\beta = 90^\circ$ as mentioned in section 2.3. Thus, the results are different for $\beta = 90^\circ$. Note that the maximum steady state axial strain (see equation (53)) for the rotating beam at $k = 0.5$ and 1 are 0.875 and 3.5 respectively. Thus, all results shown in Table 1 are only for academic interest and may be meaningless in practice.

Table 2 presents the first and second dimensionless natural frequencies for in-plane vibration ($\beta = 90^\circ$) of a slender rotating beam. The slenderness ratio of the beam considered is $\eta = 10^3$. Thus, the beam may be regarded as the Euler–Bernoulli beam. The maximum steady state axial strain (see equation (53)) for the rotating beam corresponding to $r = 1$ and $k = 0.05$ is 3.75×10^{-3} . It is seen that the results of Present-A, Present-B and those reported in the literature are in close agreement. It indicates that when the steady state axial strain is small, the effect of the Coriolis force on the natural frequencies of the rotating beam may be negligible.

Figure 4 shows the first four dimensionless natural frequencies, K_i ($i = 1, 2, 3$) and K_1^a , for the rotating beam at different angular velocities. The setting angle $\beta = 90^\circ$ and dimensionless variables $r = 0.1, \eta = 70$, and $\mu_0 = 0.32693$ are used for this example. This example was also studied by Yoo and Shin [7]. In reference [7], the beam was considered to be Euler beam. The results of the present study and reference [7] are essentially in agreement. As can be seen that as k increases, K_1^a increases for Present-A but decreases for Present-B. The K_3 and K_1^a curves cross at $k = 0.34$. The mode shapes corresponding to K_i and K_1^a are shown in Figure 5 for $k = 0.3$ and 0.4. As can be seen that at $k = 0.3$ and 0.4, the corresponding mode shapes of K_3 and K_1^a are similar. It is noted that φ_1 has appreciable change. This result may be explained as follows. Even mode shapes of w_I corresponding to K_1^a for $k = 0.3$ and 0.4 look similar, however, the slopes of mode shapes of w_I have appreciable change. The values of $w_{,x}$ and φ should be very close, because the shear strain is small in this study. Thus, the corresponding φ_I has appreciable change as well. This observation verifies that K_3 and K_1^a curves cross rather than veer at $k = 0.34$. In reference [7], it is stated that K_3 and K_1^a curves veer rather than cross at $k = 0.34$. This statement might be incorrect. It is also interesting to note that K_2 and K_1^a curves veer rather than

TABLE 2

Dimensionless frequencies for rotating Timoshenko beam ($\beta = 90^\circ, \eta = 10^3, \mu_0 = 0.32693$)

$k (10^{-3})$		$r = 0$		$r = 1$	
		$K_1 (10^{-3})$	$K_2 (10^{-3})$	$K_1 (10^{-3})$	$K_2 (10^{-3})$
0	Present-A	3.516	22.033	3.516	22.033
	Present-B	3.516	22.033	3.516	22.033
	Reference [3]	3.516	22.036	3.516	22.036
2	Present-A	3.622	22.525	4.400	23.279
	Present-B	3.622	22.525	4.400	23.279
	Reference [3]	3.622	22.528	4.401	23.282
5	Present-A	4.074	23.949	7.411	28.922
	Present-B	4.074	24.949	7.411	28.922
	Reference [3]	4.074	24.952	7.412	28.926
10	Present-A	5.048	32.118	13.257	43.224
	Present-B	5.049	32.118	13.258	43.225
	Reference [3]	5.050	32.123	13.261	43.237
20	Present-A	6.772	51.349	25.278	76.585
	Present-B	6.774	51.351	25.286	76.588
	Reference [3]	6.794	51.372	25.318	76.659
50	Present-A	10.416	116.148	61.463	181.780
	Present-B	10.437	116.175	61.584	181.824
	Reference [3]	10.899	116.200	61.641	181.936

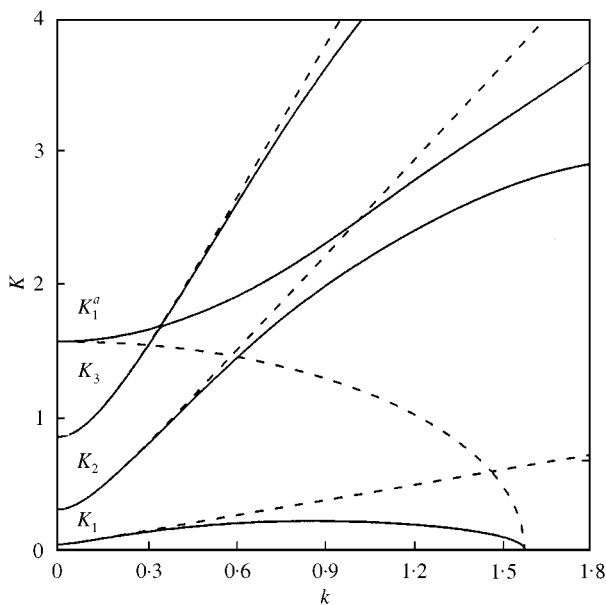


Figure 4. Variation of natural frequency with rotational speed ($\beta = 90^\circ, r = 0.1; \eta = 70; \mu_0 = 0.32693$): —, Present-A; ----, Present-B.

cross. This phenomenon might be explained as follows. When the rotation speed increases, the Coriolis force has stronger effect on the natural frequency of the lower lateral vibration mode, and the natural frequency of lower lateral vibration mode increases slower than that of the higher lateral vibration mode due to the centrifugal force. Thus, the net increase rate

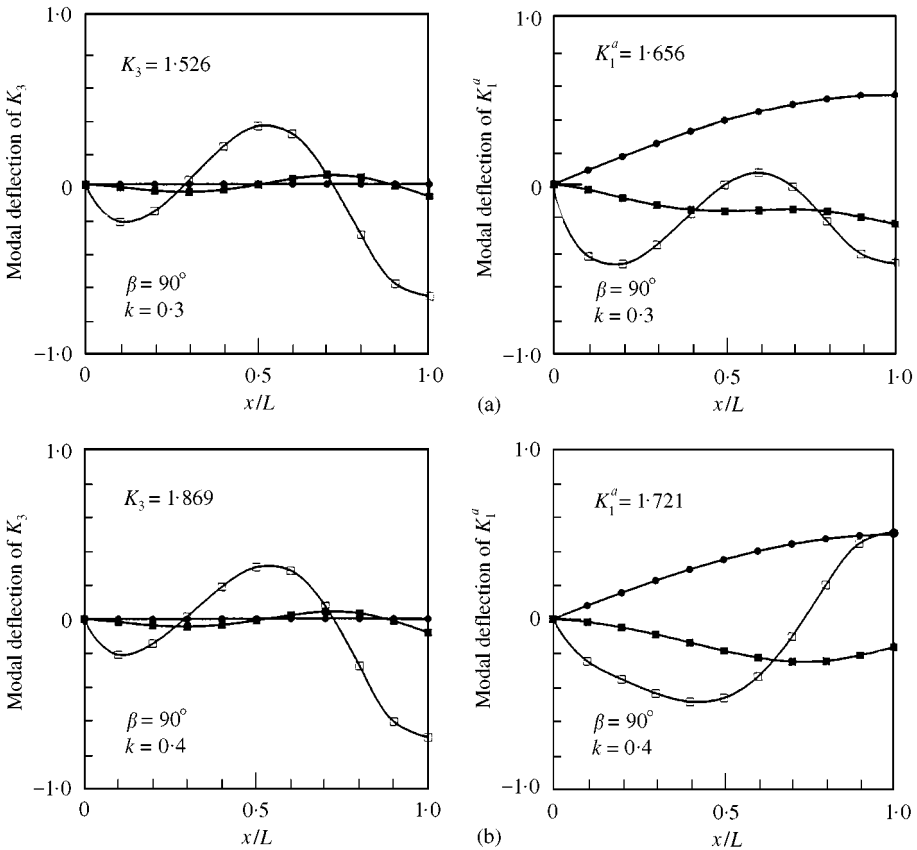


Figure 5. Variation of mode shape ($\beta = 90^\circ$, $r = 0.1$; $\eta = 70$; $\mu_0 = 0.32693$): \bullet , U_R ; \blacksquare , W_I ; \square , φ_I .

of k_2 is slower than that of k_3 with the increase of rotation speed. In order to compare the results with those given in reference [7], the frequency curves are presented for $k = 0-1.8$. However, the maximum steady state axial strain at $k = 0.2$ is 0.024. Thus, as $k > 0.2$, the results shown in Figure 4 might be meaningless.

Tables 3 and 4 present dimensionless natural frequencies K_i ($i = 1-4$) and K_i^a ($i = 1, 2$) at dimensionless rotation speeds $k = 0, 0.05$, and 0.1 for the rotating beams with different slenderness ratios. The maximum steady state axial strain (see equation (53)) for the rotating beam with $r = 0$ and 1 at $k = 0.1$ are 0.005 and 0.015 respectively. Because the Coriolis force vanishes at $\beta = 0^\circ$ and $k = 0$, the results of cases A and B are identical for $\beta = 0^\circ$ and $k = 0$. Thus, only the results of case A are presented in Tables 3 and 4 or $\beta = 0^\circ$ and $k = 0$. It is observed that for $\beta = 90^\circ$, the values of K_i^a obtained by excluding the Coriolis force are always lower than those by including the Coriolis force. As can be seen from Tables 1, 3 and 4, with the consideration of the Coriolis force, the values of K_i ($i = 1-4$) are reduced for $\eta \geq 20$. However, for $\eta = 10$, only the values of K_i ($i = 1-3$) are reduced, but the value of K_4 is increased. From equations (56) and (59), it seems that the effect of the Coriolis forces on the natural frequencies of lateral vibrations is affected by the distribution of the X_1 component of the vibrations modes, which may be affected by slenderness ratio η . However, the discrepancy between the results obtained by excluding and including the Coriolis force is insignificant for all cases presented in Tables 3 and 4. It seems that the effect of the Coriolis force on the natural frequencies of vibrating beams might be negligible.

TABLE 3

Dimensionless frequencies for rotating beam ($\mu_0 = 0.32693, r = 0$)

β	η	k	Case	K_1	K_2	K_3	K_4	K_1^a	K_2^a
0°	10	0	A	0.3231	1.4531	3.1671	4.8228	1.5708	4.7124
		0.05	A	0.3272	1.4575	3.1729	4.8295	1.5700	4.7121
		0.1	A	0.3391	1.4705	3.1902	4.8492	1.5676	4.7113
	20	0	A	0.1718	0.9570	2.3376	3.9620	1.5708	4.7124
		0.05	A	0.1800	0.9646	2.3460	3.9720	1.5700	4.7121
		0.1	A	0.2025	0.9870	2.3711	4.0019	1.5676	4.7113
	50	0	A	0.0701	0.4296	1.1640	2.1836	1.5708	4.7123
		0.05	A	0.0886	0.4476	1.1823	2.2031	1.5700	4.7120
		0.1	A	0.1285	0.4979	1.2354	2.2604	1.5676	4.7112
90°	10	0	A	0.3231	1.4531	3.1671	4.8228	1.5708	4.7124
		0.05	A	0.3230	1.4549	3.1722	4.8295	1.5748	4.7129
			B	0.3236	1.4569	3.1726	4.8294	1.5700	4.7121
		0.1	A	0.3226	1.4604	3.1876	4.8492	1.5867	4.7144
			B	0.3251	1.4681	3.1892	4.8488	1.5676	4.7113
			A	0.1718	0.9570	2.3376	3.9620	1.5708	4.7124
	20	0	A	0.1718	0.9570	2.3376	3.9620	1.5708	4.7124
		0.05	A	0.1728	0.9630	2.3453	3.9716	1.5733	4.7132
			B	0.1731	0.9634	2.3456	3.9718	1.5700	4.7121
	50	0.1	A	0.1753	0.9808	2.3684	4.0001	1.5809	4.7156
			B	0.1766	0.9825	2.3694	4.0009	1.5675	4.7113
		0	A	0.0701	0.4296	1.1640	2.1836	1.5708	4.7123
		0.05	A	0.0731	0.4474	1.1812	2.2025	1.5732	4.7131
			B	0.0732	0.4489	1.1813	2.2026	1.5700	4.7120
		0.1	A	0.0803	0.4874	1.2310	2.2580	1.5804	4.7155
		B	0.0809	0.4880	1.2316	2.2584	1.5676	4.7112	

TABLE 4

Dimensionless frequencies for rotating beam ($\mu_0 = 0.32693, r = 1$)

β	η	k	Case	K_1	K_2	K_3	K_4	K_1^a	K_2^a
0°	10	0	A	0.3231	1.4531	3.1671	4.8228	1.5708	4.7124
		0.05	A	0.3327	1.4638	3.1817	4.8395	1.5700	4.7121
		0.1	A	0.3600	1.4953	3.2247	4.8887	1.5676	4.7113
	20	0	A	0.1718	0.9570	2.3376	3.9620	1.5708	4.7124
		0.05	A	0.1904	0.9749	2.3581	3.9868	1.5700	4.7121
		0.1	A	0.2371	1.0266	2.4185	4.0600	1.5676	4.7113
	50	0	A	0.0701	0.4296	1.1640	2.1836	1.5708	4.7123
		0.05	A	0.1083	0.4707	1.2075	2.2308	1.5700	4.7120
		0.1	A	0.1782	0.5760	1.3280	2.3653	1.5676	4.7112
90°	10	0	A	0.3231	1.4531	3.1671	4.8228	1.5708	4.7124
		0.05	A	0.3286	1.4611	3.1810	4.8395	1.5749	4.7129
			B	0.3292	1.4632	3.1814	4.8394	1.5700	4.7121
		0.1	A	0.3442	1.4837	3.2221	4.8883	1.5883	4.7148
			B	0.3468	1.4929	3.2224	4.8882	1.5676	4.7113
			A	0.1718	0.9570	2.3376	3.9620	1.5708	4.7124
	20	0	A	0.1718	0.9570	2.3376	3.9620	1.5708	4.7124
		0.05	A	0.1835	0.9733	2.3574	3.9863	1.5733	4.7132
			B	0.1838	0.9737	2.3577	3.9854	1.5700	4.7121
	50	0.1	A	0.2139	1.0205	2.4158	4.0582	1.5810	4.7157
			B	0.2155	1.0225	2.4168	4.0590	1.5676	4.7113
		0	A	0.0701	0.4296	1.1640	2.1836	1.5708	4.7123
		0.05	A	0.0960	0.4680	1.2064	2.2302	1.5732	4.7131
			B	0.0961	0.4681	1.2065	2.2303	1.5700	4.7120
		0.1	A	0.1465	0.5668	1.3239	2.3630	1.5805	4.7155
		B	0.1476	0.5675	1.3245	2.3634	1.5676	4.7112	

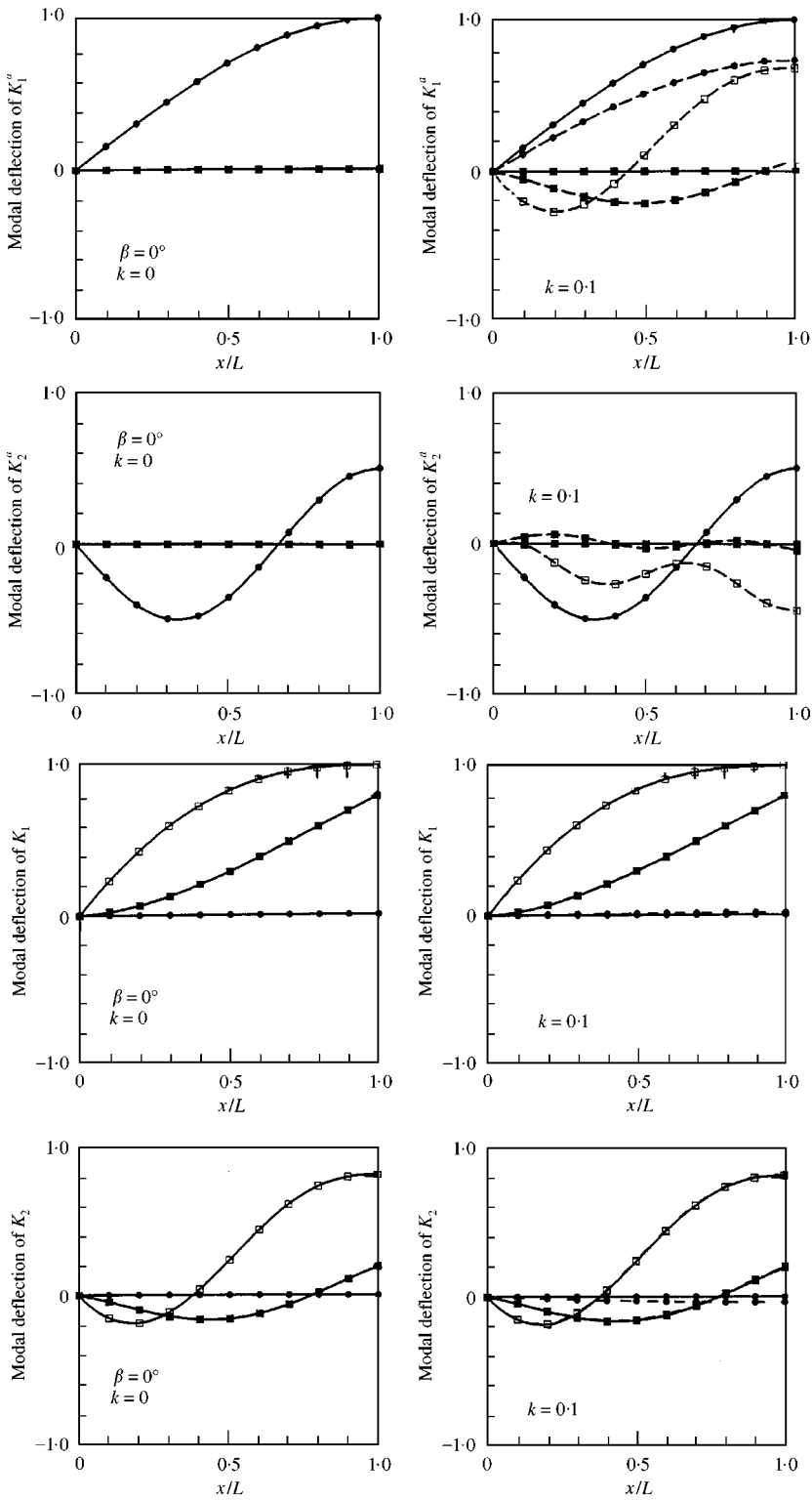


Figure 6. Mode shape of a rotating beam ($\beta = 90^\circ, r = 0; \eta = 10; \mu_0 = 0.32693$): $\bullet, U_R; \blacksquare, W_I; \square, \phi_I$ —, $\beta = 0^\circ$; ---, $\beta = 90^\circ$.

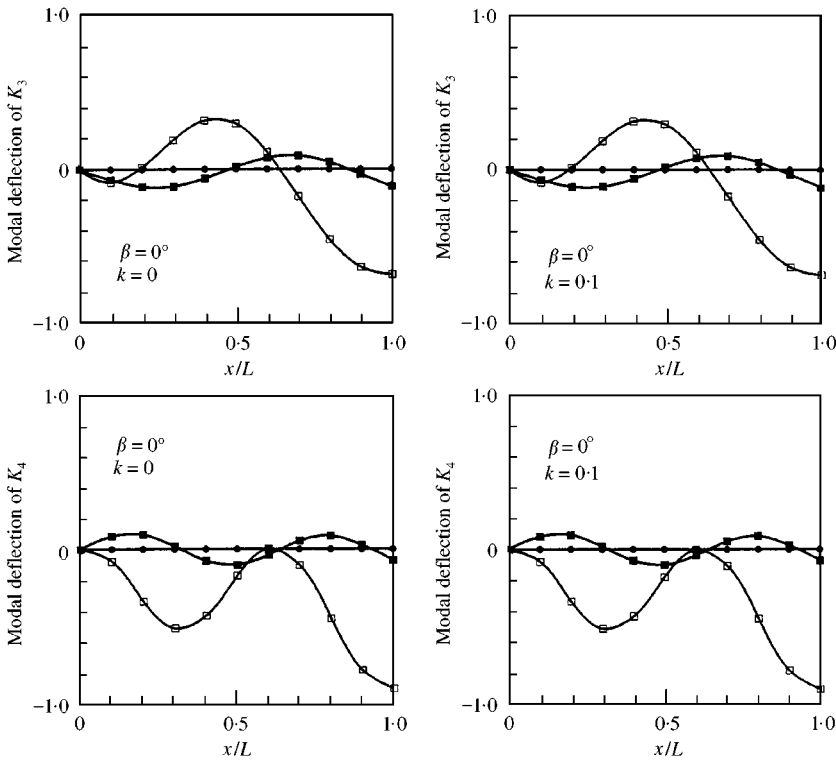


Figure 6 Continued.

As a final result, Figures 6 and 7 present the mode shapes corresponding to K_i ($i = 1-4$) and K_i^a ($i = 1, 2$) of case A at $k = 0$ and 0.1 for $\eta = 10$ and 50 given in Table 3 to illustrate the coupling between the axial and lateral vibrations of rotating beams. The mode shapes for $\beta = 0^\circ$ and 90° are identical at $k = 0$. Thus, only the mode shapes for $\beta = 0^\circ$ are presented at $k = 0$. Note that when the mode shapes for $\beta = 0^\circ$ and 90° are virtually indistinguishable at $k = 0.1$, only the mode shapes for $\beta = 0^\circ$ are presented in Figures 6 and 7. As expected, for $\beta = 0^\circ$, the axial and lateral vibrations of rotating beams are not coupled. The coupling between the axial and lateral vibrations of rotating beams can be observed from the mode shapes corresponding to K_i and K_i^a ($i = 1, 2$) at $k = 0.1$ for $\beta = 90^\circ$.

4. CONCLUSIONS

In this paper, the correct governing equations for the linear vibration of a rotating uniform Timoshenko beam are derived based on the assumptions that the beam is linear elastic and the steady state axial strain is small. The effect of Coriolis force on the natural frequency of the rotating Timoshenko beam is investigated. The vibration of the beam is measured from the position of the steady-state axial deformation, and only infinitesimal free vibration is considered. The equations of motion for rotating Timoshenko beam are derived by the d'Alembert principle and the virtual work principle. It is seen that even for linear vibration of a rotating Timoshenko beam, the exact governing equations might be derived by the consistent linearization of the fully geometrically non-linear beam theory. A method based on the power series solution is proposed to solve the natural frequency of rotating Timoshenko beam.

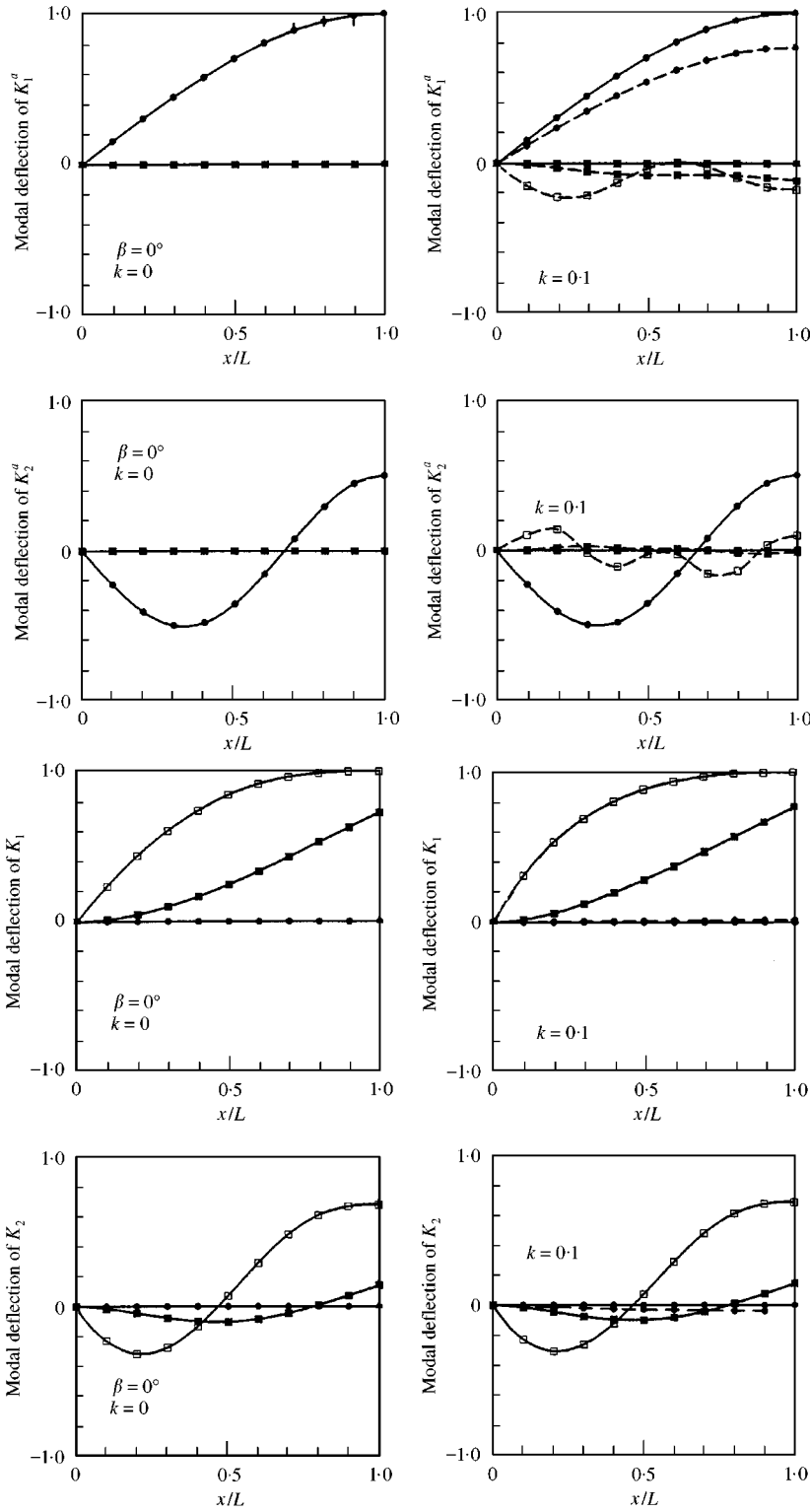


Figure 7. Mode shape of a rotating beam ($\beta = 90^\circ, r = 0; \eta = 50; \mu_0 = 0.32693$): $\bullet, U_R; \blacksquare, W_I; \diamond, \phi; \text{---}, \beta = 0^\circ; \text{---}, \beta = 90^\circ$.

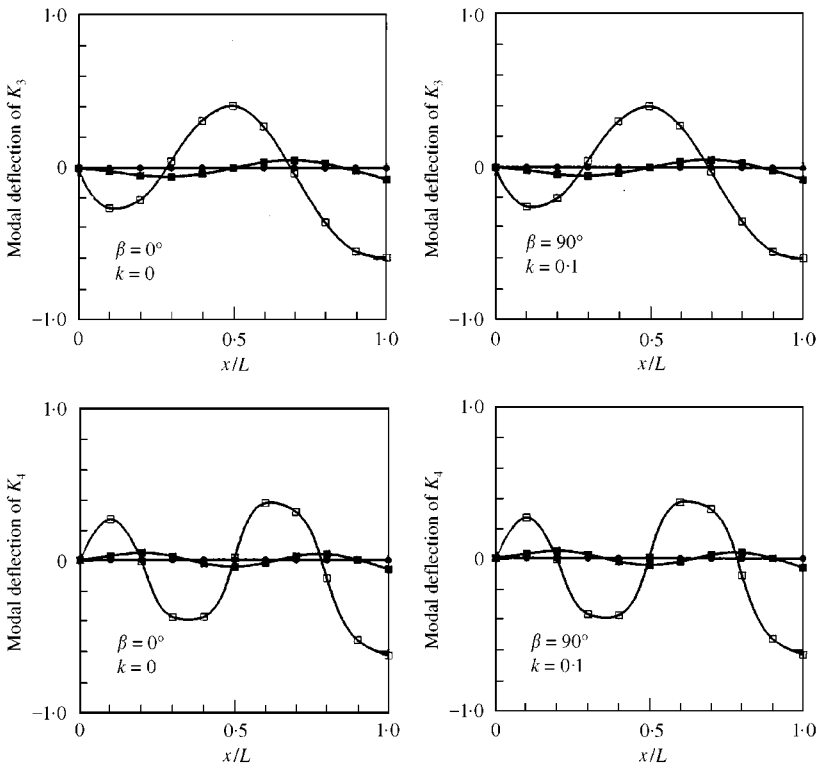


Figure 7 Continued.

The results of numerical examples show that the effect of the Coriolis force on the natural frequencies of the rotating Timoshenko beam may be negligible when the beam is linear elastic and the steady state axial strain is small. It is suggested that the value of the maximum steady state axial strain should be checked to ensure meaningful results.

Finally, it may be emphasized that, although the proposed formulation and numerical procedure are applied to the uniform rotating cantilever beams here, the method described here can be easily extended to non-uniform rotating beams with discontinuities, as well as with other end conditions.

REFERENCES

1. J. T. S. WANG, O. MAHREHOLTZ and J. BOHM 1976 *Solid Mechanics Archives* **1**, 341–365. Extended Galerkin's method for rotating beam vibrations using Legendre polynomials.
2. K. B. SUBRAHMANYAM and K. R. V. KAZA 1986 *ASME Journal of Vibration, Acoustics, Stress, and Reliability in Design* **108**, 140–149. Vibration and buckling of rotating, pretwisted precone beams including Coriolis effects.
3. T. YOKOYAMA 1988 *International Journal of Mechanical Sciences* **30**, 743–755. Free vibration characteristics of rotating Timoshenko beam.
4. S. Y. LEE and S. M. LIN 1994 *ASME Journal of Applied Mechanics* **61**, 949–955. Bending vibrations of rotating nonuniform Timoshenko beams with an elastically restrained root.
5. H. DU, M. K. LIM and K. M. LIEW 1994 *Journal of Sound and Vibration* **175**, 505–523. A power series solution for vibration of a rotating Timoshenko beam.
6. V. T. NAGARAJ 1996 *Journal of Aircraft* **33**, 637–639. Approximate formula for the frequencies of a rotating Timoshenko beam.

7. H. H. YOO and S. H. SHIN 1988 *Journal of Sound and Vibration* **212**, 807–828. Vibration analysis of rotating cantilever beams.
8. J. C. SIMO and L. VU-QUOC 1987 *Journal of Sound and Vibration* **119**, 487–508. The role of non-linear theories in transient dynamic analysis of flexible structures.
9. K. M. HSIAO 1992 *AIAA Journal* **30**, 797–804. Corotational total Lagrangian formulation for three-dimensional beam element.
10. P. W. LIKINS 1973 *AIAA Journal* **11**, 1251–1258. Mathematical modeling of spinning elastic bodies for model analysis.
11. T. J. CHUNG 1988 *Continuum Mechanics*. Englewood Cliffs, NJ: Prentice Hall.
12. D. J. MALVERN 1969 *Introduction to the Mechanics of the Continuous Medium*. Englewood Cliffs, NJ: Prentice-Hall.